A Mapping of Realistic onto Abstract Polymer Models and an Application to Two Bisphenol Polycarbonates

W. Paul*,† and N. Pistoor‡

Institut für Physik, Johannes Gutenberg Universität, D-55099 Mainz, Germany

Received October 15, 1993®

ABSTRACT: We will discuss a procedure to map atomistically detailed polymer models onto abstract polymer models like, for instance, the bond fluctuation model. This mapping is done on length and time scales mesoscopic to both models and incorporates static as well as kinetic information. The purpose of this procedure is to transfer information about a specific polymeric species into a simpler abstract model whose large scale and long time properties one can study in a computer simulation. This paper will describe the method and present an application to conformational and dynamic properties of two bisphenol polycarbonates in the melt.

1. Introduction

The computer simulation of polymers in general during the last years has more and more turned into a computer modeling of specific polymeric materials. From the beginning the simulation of polymers did heavily rely on the concept of universality.[1] Thus it suffices to simulate random walks or self-avoiding walks on lattices[2] or pearl necklace models in the continuum[3] to establish asymptotic (in chain length) and scaling properties of polymeric materials. A different question are the amplitude prefactors in these universal laws or specific small length and time scale properties that depend on a given polymeric species. Atomistically detailed models are indispensable to study the latter properties.[4,5] A successful method to study the low temperature local packing properties of bulk amorphous polymers has been the amorphous cell method by Theodorou and Suter[6] but it is a static and in principle $T = 0$ method. A dynamic simulation of polymeric properties on large length and time scales using an atomistically detailed model is hampered by severe difficulties. A single polymer chain already displays structure on length scales ranging from the bond length ($\approx$1 Å) to the coil size ($\approx$100 Å) and corresponding relaxation times for these degrees of freedom ranging from some 10^{-13} to about 10^{-5} s for long entangled chains in the melt.[7] On the technical side the simulation of these widespread length and time scales starting with all atomistic detail is out of reach of present day computer facilities, but this will of course be solved by future computer development. Even worse a molecular dynamics simulation, for instance, which would have to use a time step of about 10^{-15} s would have to be numerically stable for some 10^{10} integration steps, which is several decades above the stability limit of present algorithms.[8] Due to the nonlinearity of the equations of motion this may even pose a principal problem. The third major problem resides on the model side. Quantum chemical modeling is by now very sophisticated and can determine the energy surface for the configurations of one up to a few repeat units of a polymer (depending on the size of the unit). But it is by no means clear that there is a unique parametrization of this surface in terms of model potentials for bond lengths, bond angles, torsional angles, Lennard Jones interactions, Coulomb interactions and so forth. Thus there exist competing sets of potential parameters even for a simple polymer like polyethylene.[9–11] As these parameters are derived and tested (for instance by gas phase spectroscopy) on relatively small and isolated molecules, some sets of parameters lead to artifacts when used in the simulation of an amorphous bulk. For large scale properties, that is for the determination of the material specific prefactors in asymptotic laws, we therefore propose to use different simulational methods in the regimes where they work reliably and to define an interface between models which are suited respectively for the local microscopic and the global macroscopic properties. This will be for this exposition a quantum chemically detailed treatment on the microscopic side and the bond fluctuation model as a dynamic lattice Monte Carlo algorithm on the macroscopic side. The general ideas, however, do not depend on the choice of the abstract model and the whole procedure can of course be transfered to other models.

In section 2 we will describe the coarse-graining idea applied to derive properties on mesoscopic length and time scales where the mapping between different models is done. Section 3 will present examples for this coarse-graining done on BPA-PC[11] and describe how it can be done for the bond fluctuation model. The mapping of the bond fluctuation model onto the realistic ones is done by determining suitable energy parameters for bond length and bond angle potentials in the lattice model. This section will furthermore describe how the so posed nonlinear optimization problem is solved. Section 4 will give an application to conformational and dynamic properties of Bisphenol A polycarbonate (BPA-PC) and trimethylcyclohexane–bisphenol polycarbonate (TMC-PC) in the melt, and section 5 will summarize our conclusions.

A short account on a preliminary version of the method and the application to the glass transition of BPA-PC has been given in ref 12. A more detailed analysis of the thus determined temperature dependent viscosity and the structural relaxation of BPA-PC appeared in ref 13.

2. General Idea of the Mapping

Let us first go back to the question of universality. Imagine, for instance, a polyethylene chain in the melt and a random walk on a lattice. Examining them closely one finds a lot of structural differences, but if one steps back further and further, more and more details are no longer resolved and all that remains is a random thread whose mean squared end to end distance $\langle R^2 \rangle$ is propor-

† Present address: IBM Almaden Research Center, 650 Harry Rd., San Jose, CA 95120.

‡ Present address: IBM Deutschland Informationssysteme GmbH, AIX Systemberatungszentrum, P.O. Box 22 00 26, D-80533 München, Germany.

® Abstract published in *Advance ACS Abstracts*, February 1, 1994.

0024-9297/94/2227-1249$04.50/0

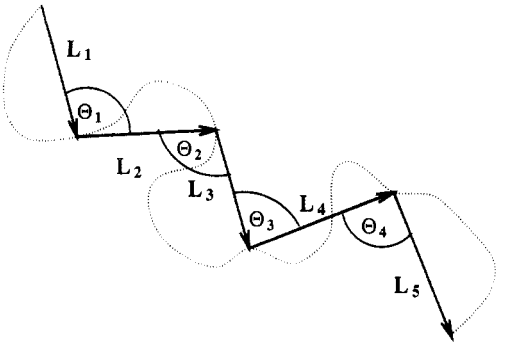

Figure 1. Illustration of the coarse-graining idea used to define bond vectors **L** on a mesoscopic scale. The dotted line represents a polymer chain and the vectors **L** connect the ends of the coarse-grained units.

tional to the number of random walk steps N along its contour.

$$\langle R^2 \rangle = \sigma^2 N \tag{1}$$

The square of the statistical segment length, σ^2, is the mean squared length of these steps. All that distinguishes polyethylene from a lattice random walk in this respect is the value of the statistical segment length. Consider furthermore the kinetics of conformational changes in these two models on length scales larger than σ and on time scales larger than the longest relaxation time of a subchain with a mean squared end to end distance σ^2. For short enough chains both are described by the Rouse model.[14] The only additional kinetic constant appearing in the Rouse model is the monomeric friction coefficient ξ or the rate constant for conformational changes

$$W = \frac{12}{\pi}\frac{k_B T}{\xi \sigma^2} \tag{2}$$

which can be derived from it. The model dependent and a priori unknown values of σ and W define what can be termed mesoscopic length scales and time scales in the respective models.

For the static properties we will apply the above described Kuhnian idea[15] of stepping along the chain with steps on a scale $L \leq \sigma$. That is, we combine m consecutive repeat units of the chain into one coarse-grained monomer and measure the distribution $P(L)$ of the end to end distances of these monomers (see Figure 1). Since L is smaller than σ the end to end vectors $\vec{L}$ are still orientationally correlated. This means that the distribution $P(\Theta)$ (Figure 1) for the angle between consecutive coarse-grained bond vectors $\vec{L}$ is not the asymptotic random walk one[16] but contains information on the polymeric species under study. The same procedure can be done with the bond fluctuation model here combining n repeat units into a coarse-grained monomer. For the microscopic model the distributions $P(L)$ and $P(\Theta)$ will depend on potential parameters for all the various degrees of freedom of the respective polymer. For the bond fluctuation model we choose model potentials for the bond lengths

$$u(l) = \tilde{u}(l - \tilde{l})^2 \tag{3}$$

and bond angles

$$v(\vartheta) = \tilde{v}(\cos\vartheta - \tilde{c})^2 \tag{4}$$

Now we require the first two moments of the distributions $\langle L \rangle$, $\langle L^2 \rangle$, $\langle \Theta \rangle$, $\langle \Theta^2 \rangle$, and $\langle L\theta \rangle$, measured in the bond fluctuation model to match those of the distributions for the realistic model. To this end we must furthermore identify the length corresponding to one lattice constant. This is done by requiring that the number density of m-mers in the realistic model (and in reality) equals the number density of n-mers on the lattice. If the simulation is done at a volume fraction (fraction of occupied lattice sites) Φ on a lattice having N sites and total volume V and it is noted that one bond fluctuation repeat unit (unit cube on a 3D simple cubic lattice) occupies eight vertices, this requirement reads

$$\Phi N/8nV = \rho/Mm \tag{5}$$

where ρ is the mass density and M the mass of a repeat unit of the specific polymer under study. The scale factor $s = (V/N)^{1/3}$ then gives the length corresponding to one lattice constant.

We have not specified how many repeat units one has to coarse grain along the realistic or the lattice model. A rule of thumb here is that the size of the coarse-grained monomers should be large compared to the mean bond length as the microscopic length scale and that the number of torsional degrees of freedom in the m coarse-grained realistic repeat units should be equal to the total number of degrees of freedom in the n coarse-grained bond fluctuation repeat units. This is a matching of the number of conformationally relevant degrees of freedom in the respective models.

Finally, we have to include information on the rate of conformational changes in the two models, to map the inner clocks in the models, in some sense. As already used before, conformational changes in a realistic polymer model are determined mainly by the torsional potentials. They are accomplished by jumps between adjacent minima in these potentials. If one knows these potentials, one can apply transition state theory to define a mean rate for the conformational changes. Let E_i be the potential energy at minimum i, ω_i the corresponding attempt frequency and $\Delta E_{ij}, j = 1, ..., n_i$ the heights of the barriers separating minimum i from its n_i neighboring minimum j. Then, the transition rate from one minimum to another is

$$\langle A \rangle = \frac{1}{Z}\sum_i \sum_{j=1}^{n_i} \omega_i \exp(-\beta E_i) \exp(-\beta \Delta E_{ij}) \tag{6}$$

with $Z = \sum_i n_i \exp(-\beta E_i)$.

This rate (or an approximation of it) has to be matched by the rate of conformational changes in the bond fluctuation model. Since the lattice model is evolving kinetically according to a Monte Carlo procedure, this rate is just given by the acceptance rate of an attempted Monte Carlo move.

The static information of the moments $\langle L \rangle$, $\langle L^2 \rangle$, $\langle \Theta \rangle$, $\langle \Theta^2 \rangle$, and $\langle L\theta \rangle$ and the rate A have to be matched between the two models, thus determining the potential parameters for the potentials chosen in the bond fluctuation model, $\tilde{u}$, $\tilde{l}$, $\tilde{v}$, and $\tilde{c}$.

3. Explicit Construction of the Coarse-Graining

The preceding section has tried to present the general idea of the mapping and was rather elusive on how it is done explicitly. It therefore applies to other abstract models as well; just exchange the term bond fluctuation with your favorite abstract polymer model. Here we now first want to show examples for the result of the coarse-graining procedure for a realistic model of BPA-PC and then explicitly construct the coarse-graining for the bond fluctuation model.

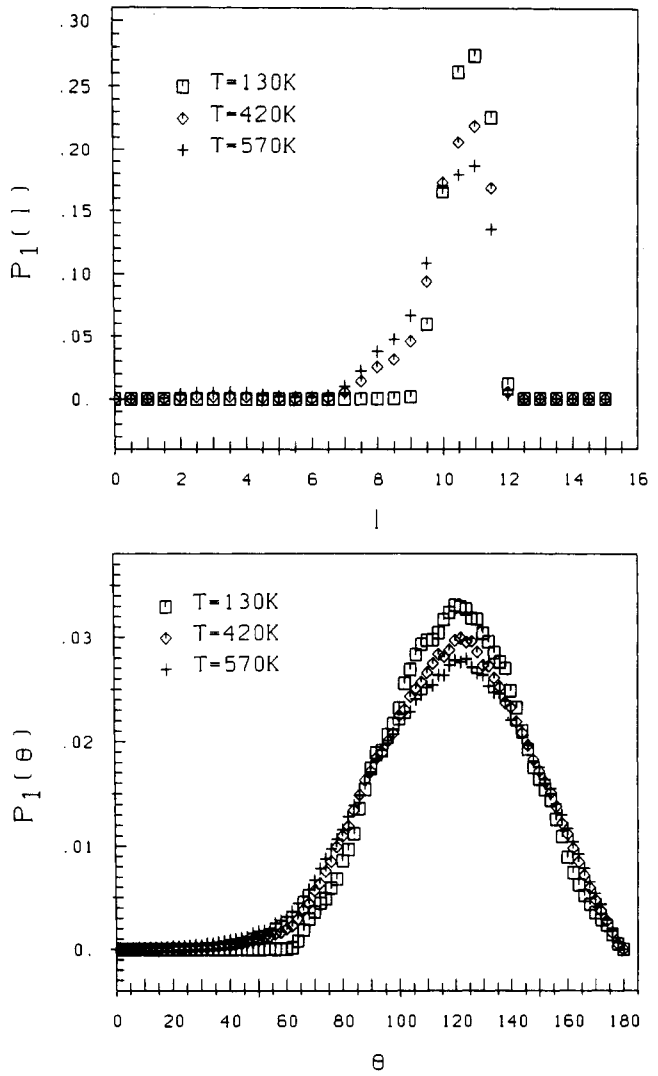

Figure 2. Distribution functions obtained for the coarse-graining applied to BPA-PC: (a) the distribution of coarse-grained bond length, $P_1(L)$; (b) the distribution of the coarse-grained bond angle, $P_1(\Theta)$.

The coarse-graining for realistic polymer models has been discussed in detail in refs 11 and 17. The starting point is a set of potential parameters that have been generated preferably by a quantum chemical ab initio calculation. With these parameters one generates a simple random walk chain drawing each degree of freedom from a distribution determined by its Boltzmann weight. This chain will have the same statistical properties as a chain in the melt or in a Θ-solvent but a different statistical segment length. The mapping we will apply to BPA-PC maps three repeat units of the lattice chain to one of the realistic model. Both coarse-grained monomers contain six conformationally active degrees of freedom. Figure 2 shows an example of $P_1(L)$ (Figure 2a) and $P_1(\Theta)$ (Figure 2b) as a function of temperature (taken from ref 11; force field parameters are given in this reference). Of course there will be a definite temperature dependence of the moments $\langle L\rangle$, $\langle L^2\rangle$, $\langle\Theta\rangle$, $\langle\Theta^2\rangle$, and $\langle L\theta\rangle$ and the rate constant A that will give rise to temperature dependent energy parameters and thus to a temperature dependent effective Hamiltonian for the simulation of the bond fluctuation model.

Concerning the kinetic information, we will approximate the mean rate of conformational changes discussed in the last section by assuming that all the attempt frequencies in the different minima of the torsional potential are equal. This way we can deal with probabilities instead of rate

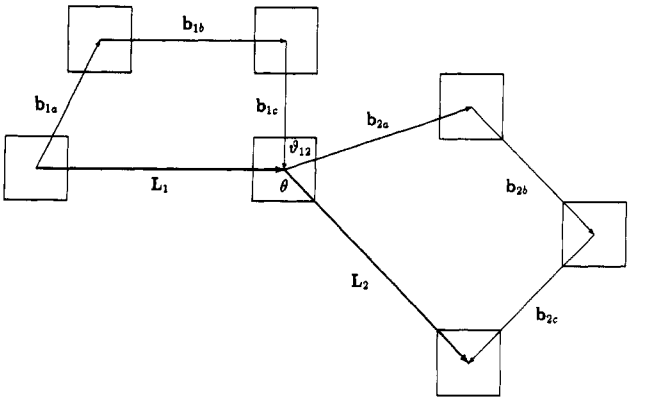

Figure 3. Illustration of the double trimer that can be enumerated exactly. Both halfs are self-avoiding and the central bond angle is not free but subject to the same self-avoidance constraints and energy parameters as the other angles.

constants which would have different units in the lattice simulation (1/MCS) and the real system (1/s). Thus the probability of a transition from one minimum to another is

$$\langle P\rangle = \frac{1}{Z}\sum_i \sum_{j=1}^{n_i} \exp(-\beta E_i)\exp(-\beta \Delta E_{ij}) \tag{7}$$

This probability defines a mean barrier $\langle\Delta E\rangle$ according to

$$\langle P\rangle = \exp(-\beta\langle\Delta E\rangle) \tag{8}$$

which is taken as an additional input value for the mapping.

This mapping is a nonlinear optimization problem with a complicated cost function that is defined as the result of a coarse-graining procedure. As the input information was generated on a chain that is a random walk on distances larger than the number of coarse-grained repeat units m (that is $m = 1$ for BPA-PC), the corresponding coarse-graining on the bond fluctuation model has to work with a random walk on distances larger than n repeat units (that is a trimer for the mapping onto BPA-PC). In general this means generating random walks of the abstract model on this length scale and measuring the required quantities on them. As a consequence, however, one would have to match two sets of data with inherent statistical errors and therefore would have to create very large samples of random walks for each set of energy parameters tested in the optimization in order to allow for a significant comparison to the target values. Fortunately, for $n = 3$ the moments of the length and angle distributions can still be determined by exact enumeration of all possible states of a double trimer; see Figure 3. Once one knows the weight function for a double trimer with trimer end to end vectors $\vec{L}_1$ and $\vec{L}_2$, $H(\vec{L}_1, \vec{L}_2)$, the required moments can be calculated, e.g.

$$\langle L\rangle = \frac{1}{Z}\sum_{\vec{L}_1,\vec{L}_2} \frac{1}{2}(|\vec{L}_1| + |\vec{L}_2|)H(\vec{L}_1, \vec{L}_2) \tag{9}$$

$$\langle\theta\rangle = \frac{1}{Z}\sum_{\vec{L}_1,\vec{L}_2} \arccos\left(-\frac{\vec{L}_1\cdot\vec{L}_2}{|\vec{L}_1||\vec{L}_2|}\right)H(\vec{L}_1, \vec{L}_2) \tag{10}$$

where $Z = \sum_{\vec{l}_1,\vec{L}_2} H(\vec{L}_1, \vec{L}_2)$. To determine the weight function, H, one has to keep in mind that the angles between bonds in the model, ϑ_i, carry an energy, $v(\vartheta_i)$, and so does the angle ϑ_{12} at the junction between the two trimers in our double trimer (see Figure 3). This means

first of all that the last bond in the first trimer and the first bond in the second one fulfill a local nonreversability condition, $(\vec{l}_{1c} + \vec{l}_{2a})^2 \geq 4$. Furthermore one has to know the weight function for a trimer configuration with a given end to end vector $\vec{L}$ and last bond $\vec{l}_c$.

$$h(\vec{L}|\vec{l}_c) = \sum_{l_a,l_b} \delta_{\vec{l}_a+\vec{l}_b+\vec{l}_c,\vec{L}} \exp[-\beta E(l_a, l_b, l_c, \vartheta_{ab}, \vartheta_{bc})] \quad (11)$$

where

$$(\vec{l}_a + \vec{l}_b)^2 \geq 4 \qquad (\vec{l}_b + \vec{l}_c)^2 \geq 4 \qquad (\vec{l}_a + \vec{l}_b + \vec{l}_c)^2 \geq 4 \quad (12)$$

Then one has

$$H(\vec{L}_1, \vec{L}_2) = \sum_{\vec{l}_{1c},\vec{l}_{2a}} h(\vec{L}_1|\vec{l}_{1c}) h(\vec{L}_2|\vec{l}_{2a}) \exp[-\beta v(\vartheta_{12})] \quad (13)$$

with the condition $(\vec{l}_{1c} + \vec{l}_{2a})^2 \geq 4$. The 108 different bonds $\vec{l}$ in the bond fluctuation model give rise to 3056 possible trimer end to end vectors $\vec{L}$ which means that $H(\vec{L}_1, \vec{L}_2)$ is a matrix with 9 339 136 elements. This has to be evaluated and summed over for each evaluation of the cost function in the nonlinear optimization procedure. To make this task numerically tractable, one has to make use of the lattice symmetry. All the trimer end-to-end vectors can be generated from a basic set of $N_{L^0} = 106$ vectors $\vec{L}_0$ fulfilling $L_x^0 \geq L_y^0 \geq L_z^0 \geq 0$ by applying one of the 48 different lattice symmetry operations S, $\vec{L} = S\vec{L}_0$. The distribution function $H(\vec{L}_1, \vec{L}_2)$ we have to determine does not depend on the orientation of the double trimer on the lattice. For all such functions f fulfilling

$$f(\vec{L}_1, \vec{L}_2) = f(S\vec{L}_1, S\vec{L}_2) \text{ for all } S \quad (14)$$

the following identity holds

$$\sum_{\vec{L}_1,\vec{L}_2} f(\vec{L}_1, \vec{L}_2) = \sum_{\vec{L}_1^0,\vec{L}_2^0} N_{\vec{L}_1^0} \sum_{S_{\vec{L}_2}} f(\vec{L}_1^0, S_{\vec{L}_2}\vec{L}_2^0) \quad (15)$$

The left hand side of this equation contains 9 339 136 terms whereas the right hand side contains only 176 346 terms. Thus the use of the lattice symmetry operations makes the exact evaluation of the static moments feasible.

In addition to the static information we must determine a mean rate of conformational changes and therefrom calculate the equivalent of a mean barrier. The conformations of the bond fluctuation chain change with a rate given by the acceptance rate of the employed Monte Carlo moves in the simulation. This can be approximated by the acceptance rate for all possible moves of the inner repeat unit in all allowed trimer configurations. If one uses Metropolis rates in the simulation this reads

$$\langle P \rangle = \frac{1}{Z} \sum_{\vec{l}_1,\vec{l}_2} \sum_{\text{moves}} \min(1, \exp[-\beta \Delta E(\vec{l}_1, \vec{l}_2, \text{move})]) \times \exp(-\beta E(\vec{l}_1, \vec{l}_2)) \quad (16)$$

where $E(\vec{l}_1, \vec{l}_2)$ is the energy of the trimer and $\Delta E(\vec{l}_1, \vec{l}_2, \text{move})$ is the change in energy associated with move, and

$$Z = \sum_{\vec{l}_2,\vec{l}_2} N_{\text{moves}}(\vec{l}_1, \vec{l}_2) \exp(-\beta E(\vec{l}_1, \vec{l}_2)) \quad (17)$$

where N_{moves} is the number of all moves principally allowed by the self-avoiding walk and bond length constraints. Again, one can define a mean "barrier" $\langle \Delta E \rangle$ by putting $\langle P \rangle = \exp(-\beta \langle \Delta E \rangle)$. This completes the description of the explicit construction of the coarse-graining for the bond fluctuation model. An equivalent level of approximation and an efficient use of the symmetry properties of the respective model for an abstract polymer chain should allow these considerations to be a guideline of how to adopt this coarse-graining procedure to other models.

Finally, one has to set up a nonlinear optimization scheme that uses the values of the moments and the mean barrier for the realistic model as target figures and minimizes a cost function which is defined as follows.

Consider the following set of variables

$$y_1 = (L - \langle L \rangle)/\sigma_L \qquad y_2 = (\theta - \langle \theta \rangle)/\sigma_\theta \quad (18)$$

where

$$\sigma_L^2 = \langle (L - \langle L \rangle)^2 \rangle \quad (19)$$

$$\sigma_\theta^2 = \langle (\theta - \langle \theta \rangle)^2 \rangle \quad (20)$$

$$\rho \sigma_L \sigma_\theta = \langle (L - \langle L \rangle)(\theta - \langle \theta \rangle) \rangle \quad (21)$$

The averages are the target values and are performed in the realistic model. Then the new variables

$$\xi_\pm = (y_1 \pm y_2)/2 \quad (22)$$

are uncorrelated and their moments in the realistic model are

$$\langle \xi_\pm \rangle = 0 \qquad \langle \xi_\pm^2 \rangle = \sigma_\pm^2 = (1 \pm \rho)/2 \qquad \langle \xi_+ \xi_- \rangle = 0 \quad (23)$$

From these the cost function is constructed:

$$\chi^2 = A(\langle \xi_+ \rangle_l^2 + \langle \xi_- \rangle_l^2) + B((\langle \xi_+^2 \rangle_l - \sigma_+^2)^2 + (\langle \xi_-^2 \rangle_l - \sigma_-^2)^2 + 2\langle \xi_+ \xi_- \rangle_l^2) + C((1 - \ln \langle P \rangle_l / \ln \langle P \rangle)^2) \quad (24)$$

where the averages $\langle \cdot \rangle_l$ are performed in the lattice model. We choose $A = B = 1$ and $C = 6$ such that statics and dynamics enter with equal weight.

Here now we have to treat the temperature dependence of the input data. There are different possibilities to take this temperature dependence into account. One possibility is to determine the potential parameters that shall be used in a simulation of the bond fluctuation model at each temperature separately. This will require a fit in a four-dimensional parameter space (for our choice of potentials) for roughly 10 different temperatures. The algorithm we use for this optimization is a simplex method taken from ref 18. The method converges reasonably fast but it may converge to different comparably good regions in parameter space for the different temperatures studied. Thus there need not be a continuous temperature variation of the fit parameters determined this way. In the next section we will show an application to the melt viscosity of TMC-PC where this leads to a large fluctuation around the mean temperature dependence. To get a smooth temperature variation of the fit parameters one has to use a different approach.

We include the temperature dependence into the energy functions by writing

$$u(l) = u_0(l - l_0)^2 + u_1(l - l_1)^2 \phi_1(\beta) \quad (25)$$

$$v(\vartheta) = v_0(\cos \vartheta - c_0)^2 + v_1(\cos \vartheta - c_1)^2 \phi_1(\beta) \quad (26)$$

where $\phi_1(\beta) = (\beta - \bar{\beta})/\overline{\beta^2 - \bar{\beta}^2}^{1/2}$ with $\bar{\beta} = (1/N)\sum_{i=1}^N \beta_i$. This

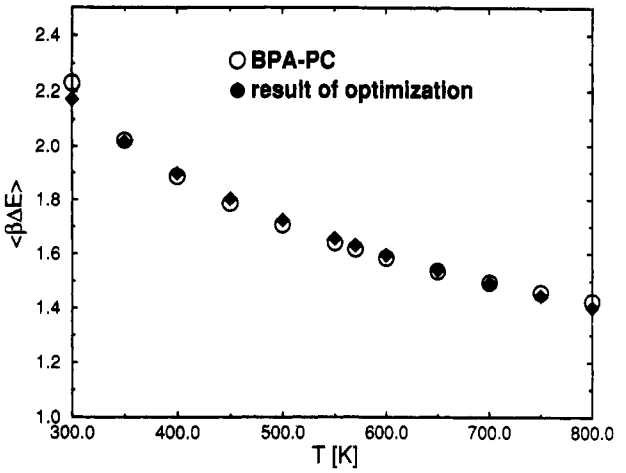

Figure 4. The mean barrier to conformational transitions as defined in the text. Open circles are the calculation from the quantum chemically determined torsional potentials for BPA-PC, and full diamonds are the values obtained from the fitting procedure.

Table 1. Parameters for the Hamiltonian Determined by a Joined Optimization for the Data at all Temperatures

	BPA-PC	TMC-PC		BPA-PC	TMC-PC
u_0	1.3625	2.2242	v_0	18.902	2.3087
u_1	0.5963	0.4113	v_1	−0.4605	−0.8087
l_0	−1.1403	0.4578	c_0	−0.6267	−0.9961
l_1	0.2136	0.9062	c_1	0.0266	0.4031

is an expansion of the temperature dependent potentials into a set of basis functions ($\phi_0(\beta) = 1$) that is orthogonal on the grid of temperatures where the input information has been given. We then have eight parameters, u_0, u_1, l_0, l_1, v_0, v_1, c_0, and c_1, which are varied in order to minimize

$$\chi^2_{tot} = \sum_{i=1}^{N} \chi^2(\beta_i) \tag{27}$$

This way one gets a smooth temperature variation of the potential parameters in the effective Hamiltonian but at the cost of an optimization in an eight-dimensional parameter space. For the numerical treatment of this optimization problem we tried two different methods so far. One is the aforementioned simplex method,[18] and the other one is Darwinian adaptive simulated annealing (DASA).[20] The efficiency and rate of convergence of the different methods depend of course on the type of optimization problem posed but also, for a given cost function, somewhat on the target values to match. For BPA-PC the simplex method achieved a $\chi^2 \leq 1$ after approximately 50 h of CPU time on an IBM RS6000/320H. For the target values given for TMC-PC the DASA algorithm proved superior although the final χ^2 value was still appreciably larger than 1. We give the best parameters determined so far in Table 1.

For both procedures the following finding holds. In the relevant temperature range the variation of the geometric moments with temperature is small compared to that of the mean barrier and, consequently, the last one influences the final values of the potential parameters most. Figure 4 shows the temperature dependence of the mean barrier in BPA-PC as determined from the torsional potential used in ref 11 and as fitted for the bond fluctuation model.

4. Conformation and Dynamic Properties in the Melt

4.1. Melt Viscosity. In this section we now want to present results obtained with the bond fluctuation model and energy parameters determined by the mapping described in the preceding section. The first application concerns the melt viscosity of BPA-PC and TMC-PC. For BPA-PC this has been discussed in refs 12 and 13 for a preliminary version of the mapping. For this application we determined the energy parameters for TMC-PC by separate fits at 10 different temperatures. These parameters were then used in a dynamic Monte Carlo simulation of the bond fluctuation model (for a detailed discussion of the method see ref 13). The simulations were performed in the Multitransputer facility of the condensed matter theory group at Mainz. We simulated 33 systems with 200 chains of length 20 each corresponding to TMC-PC oligomers at a melt volume fraction of $\Phi = 0.5$. The melts were equilibrated at each temperature and static properties (mean squared bond length $\langle l^2 \rangle$, mean squared end to end distance $\langle R^2 \rangle$, ...) as well as dynamic properties (mean square displacements, diffusion coefficient D_N, ...) were measured. These systems are well described by the Rouse theory which predicts for the viscosity

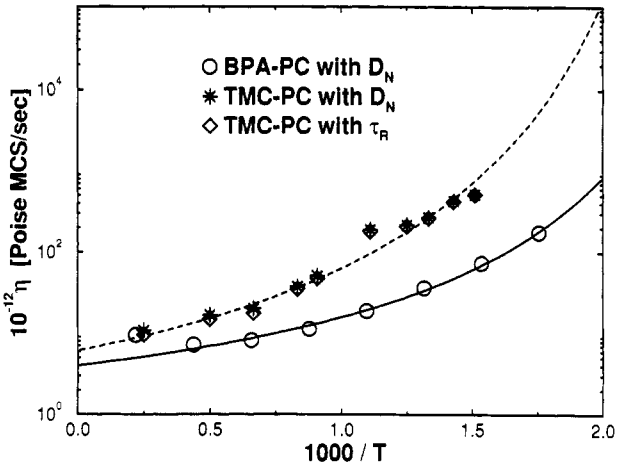

Figure 5. Comparison of the viscosity as determined by applying Rouse theory to the self-diffusion measurements in the simulation. Open circles are for a simulation using energy parameters pertaining to BPA-PC; open diamonds and stars are for TMC-PC. For the diamonds the measured diffusion constant was used as input, and for the stars the Rouse relaxation time was employed.

$$\eta = \frac{\Phi}{8s^3} \frac{k_B T}{(N-1)^2 \langle l^2 \rangle} \frac{\langle R^2 \rangle^2}{36 D_N} \tag{28}$$

where the transformation of the length scale from lattice constants to Å (scale factor s) has been accounted for.[13] The results are shown in Figure 5 in comparison to the earlier results for BPA-PC. Due to the different versions of the mapping employed the two polymers should not be compared quantitatively but at least the method captures the trend in the viscosity correctly. TMC-PC which has a glass transition at $T_g \approx 512$ K is much more viscous than BPA-PC with $T_g \approx 420$ K. Both curves are compatible with a Vogel–Fulcher behavior with a Vogel temperature of about 320 K. Note also that the data contain a still unknown time scaling from the time unit of the simulation (MCS) to real time (s). This scaling has either to be done on the mesoscopic time scales which is still an unsolved problem or—somewhat a posteriori—on the macroscopic scale equating for instance the high temperature limit of the viscosities measured in the simulation to the experimental value. This has been done in Figure 6 where we compare the behavior found in the simulation of BPA-PC to results of experiments on BPA-PC oligomers.[13] The Vogel–Fulcher temperature (321 ± 27 K) and activation energy (950 ± 113 K) predicted by the simulation are within

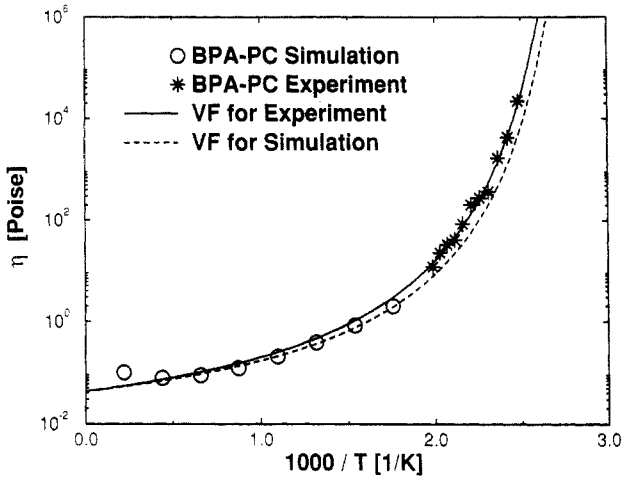

Figure 6. Comparison of the simulation results for the viscosity of BPA-PC oligomers (open circles) to the experimental findings (stars). Also shown are separate Vogel–Fulcher fits to the respective data. The Vogel–Fulcher temperature is 322 K for the experimental data and 321 K for the simulation data, and the respective activation energies are 1053 and 950 K. The prefactor for the simulation is scaled to match the curves vertically which provides a means for time scaling. One Monte Carlo step (MCS) is equal to 1.5×10^{-14} s.

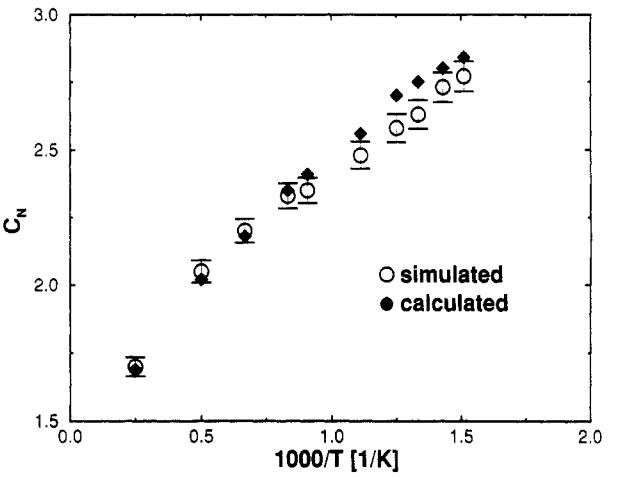

Figure 7. The characteristic ratio for a finite chain length of $N = 20$ as measured in a simulation using the energy parameters determined for TMC-PC by separate fits at the different temperatures (see text) shown as open circles. The error bars are one standard deviation. The closed diamonds are the predictions from the independent trimer approximation using the same energy parameters as input. The stiffness is here measured relative to the elementary bond length in the lattice model.

the error bars identical to the experimental findings (322 and 1053 K). The high degree of quantitative agreement of the Vogel–Fulcher temperatures is certainly fortuitous. As the simulations are done at constant volume whereas the experiments are done at constant pressure, one should expect the Vogel temperatures to differ by a few perent (T_g of BPA-PC changes by 4 deg for every 100 atm[21]). A stronger deviation is to be expected for the activation energy, and the reduction found in the simulation can be attributed to this change in ensemble. As already mentioned in the last section, we observe a strong scatter in the TMC-PC data because of the separate fits at the different temperatures (Figure 5). To avoid this scatter, one has to use the alternate optimization strategy where an assumed functional temperature dependence of the energy parameters is fitted globally to all the data at the different temperatures. We will turn to an application of the results of this optimization strategy in the following.

4.2. Independent Trimer Approximation. Before we discuss the next application, we have to introduce an approximation that allows us to calculate chain conformational properties in the melt once the energy parameters are known. The physical motivation for this approximation is the excluded volume screening under these conditions. For the bond fluctuation model at the melt density $\Phi = 0.5$ a single "blob" contains roughly one trimer of a chain. So we assume that the bond angles along the chain are uncorrelated and that the statistical properties of the chain can be calculated by using just the partition function of one trimer. This approach was shown to work extraordinarily well in a study of the stiffness dependence of various static and dynamic properties[19] in this model. In this approximation the characteristic ratio C_N is given as the simple Flory result

$$C_N = 1 - 2\frac{\langle l\rangle^2}{\langle l^2\rangle}\frac{\langle\cos\vartheta\rangle}{1+\langle\cos\vartheta\rangle} + \frac{2}{N-1}\frac{\langle\cos\vartheta\rangle - (-\langle\cos\vartheta\rangle)^N}{(1+\langle\cos\vartheta\rangle)^2} \tag{29}$$

where ϑ is defined as in Figure 3. The various averages are done using the partition function of a single trimer. To assess the validity of this approximation, we plot in Figure 7 the predicted values for C_N ($N = 20$) using the independent trimer approximation for TMC-PC and the values measured in the simulation of the TMC-PC melt. The slight discrepancy at the intermediate temperatures is probably due to a lack of equilibration of the simulated melt on the longest length scales ($\langle R^2\rangle$). On the whole the agreement is very satisfactory with a deviation of at most 5%. This means that the independent trimer approximation can even be used to make quantitative predictions for conformation dependent properties in this case. Therefore it is in principle possible to calculate all moments $\langle r_{ij}^k\rangle$ of intermonomer distances along a single chain. A direct transfer to the chain properties under Θ conditions has to be viewed with caution, since the excluded volume screening does not necessarily extend down to the trimer size[17] in that case.

4.3. Chain Stiffness in the Melt. In this final part of section 4 we want to make a direct comparison between the prediction for $C_\infty(T)$ for BPA-PC and TMC-PC in the melt using the same mapping procedure for both polymers. With the form (25) for u and v we have fitted data for moments measured on the two polycarbonates. We use the resulting parameter functions as input for the independent trimer approximation and calculate for instance $C_\infty(T)$ for melt chains according to eq 29. Figure 8 shows our results for both polymers in the temperature region from 300 to 600 K. For both polymers the statistical segment length is slightly larger than the repeat unit. These results would suggest that TMC-PC is stiffer than BPA-PC in the high temperature limit but shows a less pronounced variation with temperature. Note, however, that the parameter values available for TMC-PC are not as good as those for BPA-PC so that this result should be regarded as an educated guess. Furthermore both curves are intercepted by the glass transition of the respective material, so that the curve for BPA-PC should level off to a glass value somewhere between 350 and 420 K and the one for TMC-PC somewhere between 450 and 512 K depending on the time scale of the experiment. For BPA-PC there is experimental information available for the radius of gyration of the chains in the glass.[22] For chains of a weight average molecular weight of $M_w = 49\,000$ the radius of gyration was found to be $\langle R_g^2\rangle^{1/2} = 32.34$ Å.

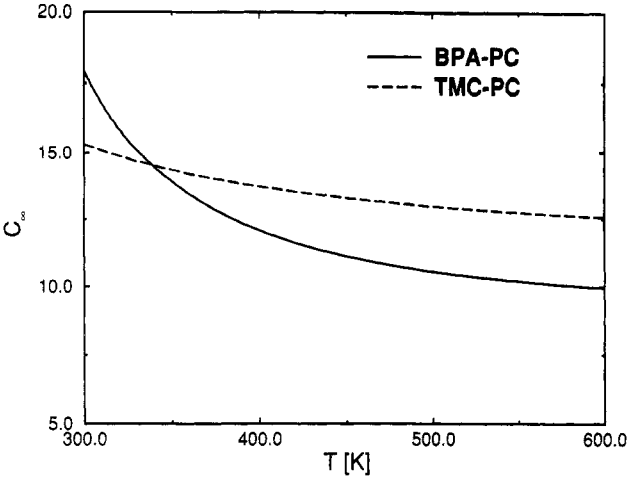

Figure 8. Comparison of the independent trimer prediction for the infinite chain length characteristic ratio for BPA-PC and TMC-PC.

Assuming Gaussian chain statistics, we would deduce a characteristic ratio as measured on a chain of 193 repeat units

$$C_N \doteq \frac{\langle R^2 \rangle}{\tilde{N}\bar{l}^2} = 13.6 \qquad (30)$$

Here $\tilde{N}$ is the number of backbone bonds in the chain and $\bar{l}^2 = 1.99845$ Å^2 is the averaged squared length of these bonds.[11] The predicted curve for the characteristic ratio of BPA-PC reaches this value somewhere around 360 K. This shows that the overall chain geometry could be successfully transferred from the microscopic input information into the lattice model.

5. Conclusions

We have shown in this paper how to define an interface between descriptions of polymers on different levels of abstraction. Such an interface is needed for the computer modeling of the behavior of specific polymers on all the length scales and time scales a typical polymer displays. Very naturalistic models should be used for the investigation of local processes on short length and time scales. Large scale relaxation exceeding the local one easily by 8–10 orders in time scale is better studied using abstract models. We have shown how to incorporate information on the chain structure and dynamics on a mesoscopic level into the simulation of an abstract model, in our case the bond fluctuation lattice model. The procedure outlined is, however, generally applicable. This method can be used to predict phenomenological constants in macroscopic laws that are universally applicable to polymeric substances irrespective of their specific structure. One such law is the Vogel–Fulcher law for the viscosity of a polymer melt as one approaches the glass transition. We have shown simulation results for the melt viscosity of two structurally different bisphenol polycarbonates. For Bisphenol A polycarbonate our results that were obtained for oligomers were checked by experiments and a high degree of agreement was found. A second application considered the characteristic ratio of chains in the melt. For the bond fluctuation model a simple theoretical approximation is possible to calculate this from the Hamiltonian optimized to model a specific polymer. The results are again in reasonable agreement with experimental data on these polycarbonates. The numerical treatment of the nonlinear optimization problem that is posed by the above mentioned mapping between a detailed and an abstract model is computationally involved and needs further study for the determination of the best optimization algorithm. The results found so far show, however, that the defined interface contains the necessary information for the discussed applications. Macroscopic quantities depending on the interchain interaction will need an extension of the mapping to include this feature also into the lattice model. A further effort is also needed to incorporate information on the polydispersity of the polymer sample into the modeling.

Acknowledgment. It is a pleasure to acknowledge a fruitful collaboration with K. Binder, K. Kremer, and D. W. Heermann that got this work started. We thank I. Batoulis and B. Pittel for informing us about the results of their quantum chemical calculations on monomers of BPA-PC and TMC-PC which were used as input in the mapping procedure. Furthermore financial support by the German Federal Ministry of Research and Technology under Grant 03M4028 and by BAYER is greatfully acknowledged.

References and Notes

(1) De Gennes, P. G. *Scaling Concepts in Polymer Physics*; Cornell University Press: Ithaca, New York, 1979.
(2) Kremer, K.; Binder, K. *Comp. Phys. Rep.* **1988**, *7*, 259.
(3) Baumgärtner, A. *Annu. Rev. Phys. Chem.* **1984**, *35*, 4.
(4) Smith, G. D.; Jaffe, R. L.; Yoon, D. Y. *Macromolecules* **1993**, *26*, 298.
(5) Yoon, D. Y.; Smith, G. D.; Matsuda, T. *J. Chem. Phys.* **1993**, *98*, 10037.
(6) Theodorou, D. N.; Suter, U. W. *Macromolecules* **1986**, *19*, 379 and references cited therein.
(7) Binder, K. *Macromol. Chem., Macromol. Symp.* **1991**, *50*, 1.
(8) Haile, J. M. *Molecular Dynamics Simulation*; Wiley: New York, 1992.
(9) Ryckaert, J. P.; Bellemans, A. *Chem. Phys. Lett.* **1975**, *30*, 123; *Faraday Discuss. Chem. Soc.* **1978**, *66*, 95.
(10) Yoon, D. Y.; Flory, P. *J. Chem. Phys.* **1974**, *61*, 5366.
(11) Baschnagel, J.; Binder, K.; Paul, W.; Laso, M.; Suter, U. W.; Batoulis, I.; Jilge, W.; Bürger, T. *J. Chem. Phys.* **1991**, *95*, 6014.
(12) Paul, W.; Binder, K.; Kremer, K.; Heermann, D. W. *Macromolecules* **1991**, *24*, 6332.
(13) Paul, W. In *Slow Dynamics in Condensed Matter*; Kawasaki, K., Tokuyama, M., Kawakatsu, T., Eds.; AIP Conference Proceedings 256; AIP: New York, 1992. Paul, W.; Binder, K.; Batoulis, J.; Pittel, B.; Sommer, K. H. *Macromol. Chem., Macrom. Symp.* **1993**, *65*, 1.
(14) Rouse, P. E. *J. Chem. Phys.* **1953**, *21*, 1272.
(15) Kuhn, W. *Kolloid.-Z.* **1936**, *76*, 258; **1939**, *87*, 3.
(16) Laso, M.; Öttinger, H. C.; Suter, U. W. *J. Chem. Phys.* **1991**, *95*, 2178.
(17) Baschnagel, J.; Quin, K.; Binder, K.; Paul, W. *Macromolecules* **1992**, *25*, 3117.
(18) Press, W. H.; Flannery, B. P.; Teukolsky, S. A.; Vetterling, W. T. *Numerical Recipes*; Camebridge University Press: New York, 1986.
(19) Wittmer, J.; Paul, W.; Binder, K. *Macromolecules* **1992**, *25*, 7211.
(20) Montoya, F.; Dubois, J.-M. *Europhys. Lett.* **1993**, *22*, 79.
(21) *Encyclopedia of Polymer Science and Engineering*, 2nd ed.; Wiley: New York, 1989; Vol. 7.
(22) Gawrisch, W.; Brereton, M. G.; Fischer, E. W. *Polym. Bull.* **1981**, *4*, 687.